

Automated Visual Inspection Algorithm for Solder Joint of Surface Mount Devices Based on Three-Dimensional Shape Analysis

Toshifumi Honda^{†1}, Yukio Matsuyama^{†1}, Hisae Yamamura^{†1}, Hideaki Sasazawa^{†1},
Takanori Ninomiya^{†1}, Ludwig Listl^{†2}, Anton Schick^{†2} and Richard Schneider^{†2}

^{†1}Production Engineering Research Laboratory, Hitachi Ltd.
292 Yoshida-cho, Totsuka-ku, Yokohama 244, Japan
E-mail: 39honda@perl.hitachi.co.jp

^{†2}Corporate Production and Logistics, Siemens AG.
Otto-Hahn-Ring 6 D-81739 Munich, Germany
E-mail: richard.schneider@zfe.siemens.de

Abstract

An automated visual inspection system has been developed for use with surface mount devices (SMDs) on a printed circuit board (PCB). The system is capable of inspecting minute solder joints of fine pitch components as small as 0.3mm pitch QFP leads. A solder joint is judged using a height image and an intensity image that are detected by a unique confocal height sensor. A solder joint is classified based on the extracted features of solder fillet shape and correlation between a lead and its pad position. Therefore, accurate recognition of these components from the images is extremely important for reliable inspection. However, the shape of a solder fillet varies greatly, depending on factors such as the soldering process, material of the lead and the solder itself. Furthermore, the height sensor sometimes detects erroneous height data, observed as spike noise caused by insufficient reflection light from the inclined specula surface of a solder fillet. The present authors developed a unique noise reduction algorithm that utilizes a model shape of a solder joint as well as a statistical edge detection algorithm based on highest probability to recognize a solder joint without influence of noise. Each component of a solder joint is recognized by a method customized for the type of it, in order to achieve reliable recognition of various shapes of solder joints. Evaluation of the system confirms that it realizes a 100% defect detection rate and a very low false alarm rate (0.16%). The present paper describes the employed inspection algorithm and briefly explains the developed automated inspection system.

1. Introduction

The continuing trend toward smaller sized PCBs and higher component density has been accelerated by the popularization of personal data terminals such as notebook computers and portable telephones. Since soldering cannot be guaranteed to be free of defects, visual inspection of solder joints is indispensable. However, visual inspection by a human operator has become more difficult as components of finer pitch has been increasingly mounted on PCBs.

Various kinds of automated solder joint inspection techniques have been reported to date¹⁾⁻⁵⁾. With the exception of the X-ray method, commercially available solder inspection systems can be roughly classified into two categories according to the inspection method: a multi-level tiered illumination approach and a triangulation method.

The tiered illumination method⁶⁾⁻⁷⁾ can detect the inclination angle of a target surface by illuminating the

surface from various incident angles and detecting reflected light; usually from above the target surface. A variant of this system uses the same principle but illuminates the joint surface using a laser beam positioned above the solder joint and detects reflected light from various angles⁸⁾. Since these methods detect 3-D shapes indirectly based on a surface inclination, they have the inherent limitation of being unable to detect surfaces that incline more than 45° or those that have steps; they can only detect 3-D shapes of gentle portions of a solder fillet and cannot measure lift of lead, which is necessary for detection of the no-connection defect.

The laser triangulation method⁹⁾ can detect the 3-D shape of a target directly but it has a inherent problem of secondary reflection which may cause inaccurate detection of height of a specula surface.

Moreover, both of the methods are affected by the problem of a dead angle; i.e. light reflected from a fillet is obstructed by the body of a component in the view field of the detector. Because of poor performance of 3-D shape acquisition, to inspect solder joints using existing systems based on 3-D shape analysis has been difficult. As a result, existing systems must rely on analysis of intensity patterns for judgment of a solder joint. Since an intensity image is severely influenced by various soldering conditions, conventional inspection algorithms cope with the change of intensity image by modifying inspection parameters. However, each time production conditions are changed, these methods require time to optimize the parameters. Thus in actual production line, they often fail to contribute to the quality assurance of PCBs.

This problem has been overcome by development of an automated solder joint inspection system based on 3-D shape analysis. A newly developed confocal height sensor has been applied to detect 3-D shape accurately without influence of secondary reflection. The developed algorithm analyzes features of detected three-dimensional shapes very precisely and judges defects based on understandable physical values of 3-D shape features.

2. Objects of inspection and technical issues

The objects of inspection are SMDs such as chip components as small as 1005 size (1.0mm×0.5mm) and gull wing lead components such as QFPs (Quad Flat Packages) and SOPs (Small Outline Packages) whose lead pitch is as small as 0.3mm pitch. Figure 1 shows typical defects to be detected including lead misplacement, no connection, bridge and insufficient solder. The ability to

detect these defects through their three-dimensional shape is essential.

The major technical issue concerning an inspection algorithm is to realize accurate and reliable inspection of various types of solder joints based on three-dimensional analysis. Solder joints vary in shape depending on various soldering conditions, such as the soldering process, the quantity of solder and the presence of flux. However, the algorithm should allow inspection without modification of inspection parameters, thus making the system applicable to many kinds of PCBs in an actual production line. Furthermore, detected height image sometimes includes noise. Therefore, the algorithm should enable robust and precise recognition of various shapes of a solder joint without using data regarding soldering conditions in order to realize reliable inspection performance.

3. 3-D shape detection

Figure 2 shows the principle of the confocal microscope. A pin hole is set at a conjugate position of an objective's focal position so that only light which passes through the pin hole is detected by a sensor. When a target surface is at the objective's focal position, light reflected from the target surface focuses at the pin hole. Therefore, all the light passes through the pin hole, and can be detected by the sensor. However, when the target surface lies outside the objective's focal plane, reflected light is focused in front of or behind the pin hole, and as a result only a portion of the reflected light can be detected through the pin hole.

From this principle, one can deduce that when a target having a complex shape is detected, the portion of the target lying in the objective's focal plane is detected as being brighter than the other portions. In other words, the height associated with the bright area in the detected image can be identified. Using this method to identify height in the image is time consuming because plural images should be acquired at different heights of a target.

In order to shorten the image acquisition time, a new detection method using the confocal principle has been developed (Figure 3). In this system, the target surface is illuminated by a narrow-focus laser beam. Several pin hole/sensor pairs are set at different focusing positions corresponding to different target heights, and the sensors detect the reflected light simultaneously. The height corresponding to the sensor that detects the maximum intensity is regarded as the target height. This can be used to obtain resolvable height steps of equal in number to the sensors. Height resolution has been increased by assuming that each sensor's output can be plotted to obtain a Gaussian function as shown in Figure 3, where the peak of the Gaussian function corresponds to the target height. In addition to the height value, the maximum intensity of all the sensors is outputted as intensity value.

The illuminating laser spot is scanned by a polygonal mirror oriented in the X-direction. By moving the Y-stage perpendicular to the paper, the entire 3-D shape of a target is determined.

4. Image processing algorithm

Under normal conditions, the detected images of a solder fillet, especially the intensity image, are heavily influenced

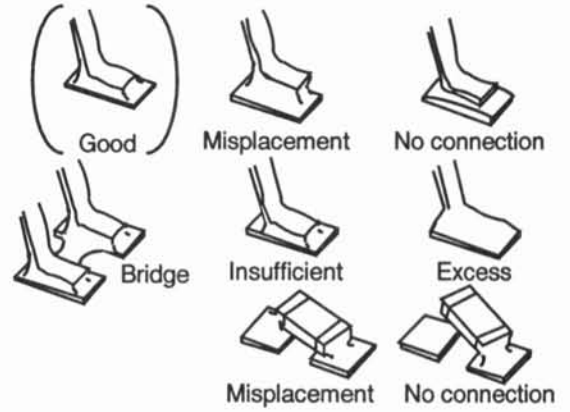


Figure 1 Typical soldering defects

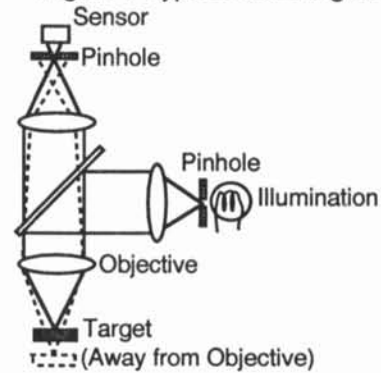


Figure 2 Principle of confocal microscope

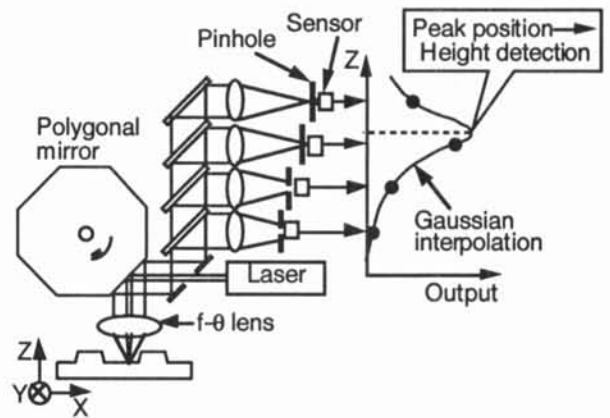


Figure 3 Principle of 3D image detection method

by factors such as the soldering process, component type, material of the lead and of the solder itself, the quantity of solder, oxidation of the solder fillet and the presence of flux. Therefore, the detected height image is primarily used for recognition of the solder joint, and the intensity image is used for increasing reliability.

Figure 4 shows the flow of the developed algorithm. Based on CAD data, an image processing window is set to include one solder joint. The developed algorithm is applied to each window to recognize the lead, pad and solder fillet. Subsequently the solder joint is evaluated according to physical criteria such as fillet length, width and height, misplacement of the lead from its pad, lift of the lead and steepness of the solder fillet (Figure 5). The following section describes the developed image processing techniques and defect judgment algorithm.

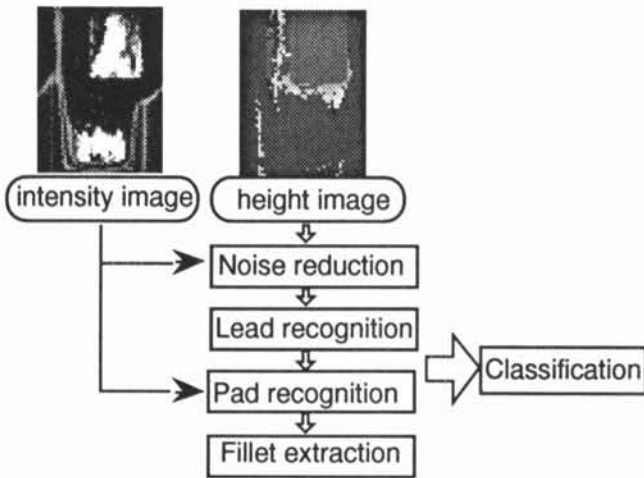


Figure 4 Algorithm flow

4.1 Image processing techniques

This sub section describes two developed image processing techniques; noise reduction and edge detection. These techniques enable reliable recognition of various shapes of solder joints even when noise pixels are present in a height image.

(A) Noise reduction

Since connection between a lead and a pad is judged based on its toe shape, accurate recognition of toe fillet shape is extremely important for reliable inspection of fine-pitch-lead LSIs. Because of insufficient light reflected from the specula surface of a solder fillet, the height sensor sometimes detects erroneous height data, observed as spike noise. Spike noise is detected especially at the connection between a lead and a solder fillet because the reflection from the steep surface of the solder fillet is very weak. Because the noise widely spreads in the vicinity of a lead, conventional techniques such as employing a median filter are not effective in eliminating noise pixels. Our algorithm distinguishes noise pixels from pixels depicting true height by comparing the height of pixels with a rough 3-D model of the solder joint. Subsequently, an improved median filter is applied to eliminate recognized noise pixels.

This process has the following features:

- (1) Recognition of noise pixels based on a rough model of

the solder joint in order to prevent removal of correct height pixels upon removal of noise pixels.

- (2) Intensity image is used to avoid enlarging/shrinking a region (e.g. lead or fillet) by substitution of noise pixels.

As shown in Figure 6 (a), noise appears outside the edge of the lead. Therefore, the conventional median filter may enlarge the length/width of the lead and this may lead to misunderstanding of the lead position. Furthermore, this may increase the number of noise pixels (Figure 6 (b)), thus degrading detection of the 3-D shape of the fillet.

The developed algorithm overcomes this problem by using the intensity image. The procedure is as follows;

- (a) Detect rough lead height and PCB height using a histogram of the height image.
- (b) Recognize a pixel as noise if its height is considerably higher than the lead height or considerably lower than the PCB height.
- (c) For each noise pixel, extract neighboring pixels whose intensity value are similar to that of the noise pixel and whose height values are not recognized as noise. Change the height value of the noise pixel to the median height value of the extracted pixels. If no neighboring pixels satisfy the above condition, do not change the height value of the noise pixel.
- (d) Repeat step (b) and (c) until no pixels in the height image are changed.

The above algorithm can decrease noise at the solder fillet (Figure 6 (c)), thus enabling accurate edge detection from the height image.

(B) Edge detection

Some noise pixels may remain in the height image even after being subjected to the noise reduction process. Therefore, a statistical edge detection algorithm that can detect an edge without being influenced by noise has been developed. This method can also be employed to determine the edge of a segment whose pixel values are not very stable, such as an intensity image of a pad. This is usually detected as bright; however, intensity may be reduced depending on various conditions such as solder fillet shape or oxidation.

The developed algorithm determines an edge position to exist at a location where the probability of existence of an

Lead characteristics $H < Th_h$ $L > Th_l$ $M < WL \times Th_m$ $(CL > Th_{cl1} \cup$ $(CL > Th_{cl2} \cap \theta > Th_\theta))$	 Standard type	 Special type	
Chip characteristics $H < Th_h$ $L > Th_l$ $W > Th_w$ $M < WL \times Th_m$ $(CL > Th_{cl1} \cup$ $(CL > Th_{cl2} \cap \theta > Th_\theta))$	 Small type	 Large type	 Large type (2 electrodes) $W = W1 + W2$

Figure 5 Criteria for satisfactory solder joints

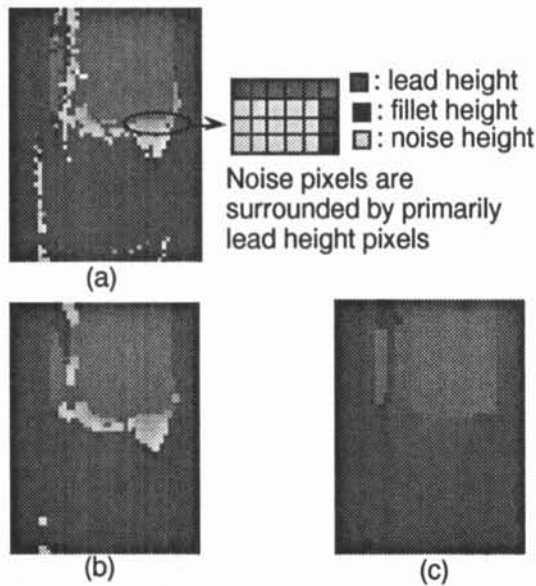


Figure 6: (a) Originally detected height image. (b) Image filtered by conventional median filter. (c) Image filtered by developed filter.

edge reaches a maximum. The probability of a pixel belonging to the target is assumed to be expressed by the following sigmoid function (Figure 7).

$$P(\hat{i}(x)=1) = \frac{1}{1 + e^{-\frac{i(x)-Th}{T}}} \quad (1)$$

- where $i(x)$: pixel value
- $\hat{i}(x)$: If the pixel belongs to the target, this value is set to 1, otherwise this value is set to 0.
- Th : threshold value
- T : parameter to decide shape of the sigmoid function

In this assumption, the probability of a pixel belonging to the target exceeds 50% when its pixel value exceeds threshold value, Th .

As an example, let's consider edge detection of a profile shown in Figure 8. When the edge position, X_e , is equal to x_2 , the value of $\hat{i}(x)$ must be 0 between x_1 and x_2 and must be 1 between x_2 and x_3 . Therefore, probability of this occurrence, $P(X_e = x_2)$, is calculated using the following expression.

$$\begin{aligned} \ln P(x_e=x_2) &= \ln \left(\prod_{x=x_1}^{x_2-1} (1 - P(\hat{i}(x)=1)) \prod_{x=x_2}^{x_3} P(\hat{i}(x)=1) \right) \\ &= -\frac{1}{T} \sum_{x=x_1}^{x_2-1} (i(x)-Th) - \sum_{x=x_2}^{x_3} (1 + e^{-\frac{i(x)-Th}{T}}) \end{aligned} \quad (2)$$

Since the second term is constant for a given value of x_2 , the maximum probability, $P(x_e=x_2)$ is calculated based on only the first term. Therefore, edge position, x_2 , is determined as the point where the following expression reaches its maximum value.

$$\sum_{x=x_1}^{x_2-1} (Th - i(x)) \quad (3)$$

The profile shown in figure 8 includes intervals located to the right side of the actual edge where the value of the profile is below the threshold value. Conventional algorithms may misdetect the edge because of influence from those intervals. The developed algorithm can achieve

reliable edge detection by maximizing probability of the occurrence.

Following edge detection, a local interval is designated as the recognized edge is located at the center of this interval and all the pixel values within the interval are approximately equal to Th . The actual edge is finally recognized within the interval where the slope of the profile reaches a maximum.

Figure 9 shows a result of edge detection from an intensity image. The developed algorithm could detect the edges even when the conventional binarization method could not.

4.2 Defect judgment algorithm

This section describes the processing of each defect judgment algorithm.

(A) Recognition of lead

Lead location is determined by detecting toe edge and side edges of the lead from a height image. A misplacement defect can be judged by the amount of overhang of the lead tip in relation to its pad. Therefore, the algorithm first determines the toe edge of the lead, then determines the side edges of the lead from the image in the vicinity of the detected toe edge.

A large quantity of solder may hide the toe edge of a lead in a height image. In order to be usable for detecting edges of various shapes of solder fillets, the algorithm detects lead toe edge based on the differential of gradient angle at a lead and at a solder fillet, as shown in Figure 10 (a). The toe edge is recognized as the position where the differential of an angle, θ , reaches its smallest value. The algorithm finds the position using the coordinate transform method instead of using trigonometric functions which would consume a large quantity of computational power. In order to calculate the differential of the gradient at a point, the algorithm determines two tangent vectors, one to the left and one to the

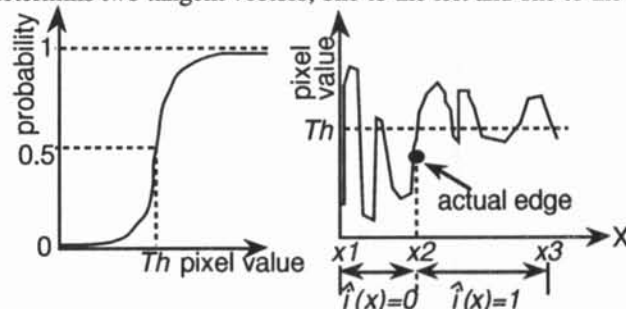


Figure 7 Sigmoid function Figure 8 Edge detection

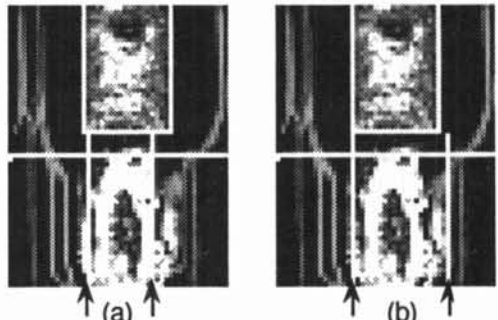


Figure 9: (a) Pad edge detected by conventional binarization method. (b) Edge detected by developed algorithm

right of the point, as shown in Figure 10 (a). In order to evaluate the angular difference of angle between two tangent vectors, \mathbf{a} and \mathbf{b} , we employ a u - v coordinate space wherein the abscissa is parallel with \mathbf{b} . In u - v coordinates, the vector \mathbf{a} is expressed as \mathbf{a}' , which is calculated using the following expression.

$$\begin{pmatrix} a'_u \\ a'_v \end{pmatrix} = \frac{1}{|\mathbf{b}|} \begin{pmatrix} b_x & b_y \\ -b_y & b_x \end{pmatrix} \begin{pmatrix} a_x \\ a_y \end{pmatrix} \quad (4)$$

The toe edge is detected at the position where the value of a'_v/a'_u reaches a maximum. This method enables reliable determination of an unclear edge of a lead toe.

Since the side of a fillet is very steep and the light reflected from that portion is of low intensity, detected height data sometimes contains much noise at that portion. When the noise covers a large region, the employed noise filter cannot completely remove noise. Therefore, a robust edge detection algorithm is necessary for reliable determination of side edges of a lead. The developed edge detection algorithm previously explained is employed for reliable detection of side edges from height images.

(B) Recognition of pad

The detected pad image is greatly influenced by the quantity of solder. As shown in Figure 11 (a), the pad is visible in an intensity image when the quantity of solder is small. Contrast between pad and the surrounding area in a height image is low compared with that in an intensity image. However, as shown in Figure 11 (b), when the quantity of solder is large, the pad is covered by solder fillet and is invisible. Therefore, the developed algorithm checks a pad in order to determine whether its surface is visible or covered by solder. The algorithm first attempts to recognize pad edges from an intensity image, and if this fails, the pad edges are detected from a height image.

Because a visible pad is detected as being bright, a bright region in an intensity image is recognized as being a pad. However, the intensity of the pad is greatly influenced by fillet shape, oxidization, or the presence of flux. Therefore, a robust algorithm is necessary for determination of pad edges. The edge detection technique explained previously is employed in order to increase robustness. If the distance between the detected pad edges is shorter than design pad width, then the pad is considered to be invisible.

In edge detection from a height image design pad width is referred to in order to avoid influence by other edges in the vicinity of a pad such as a resist edge (Figure 11 (d)). Initially, threshold height is determined based on the detected PCB substrate height and the assumption that the pad edge cannot be much higher than the PCB substrate.

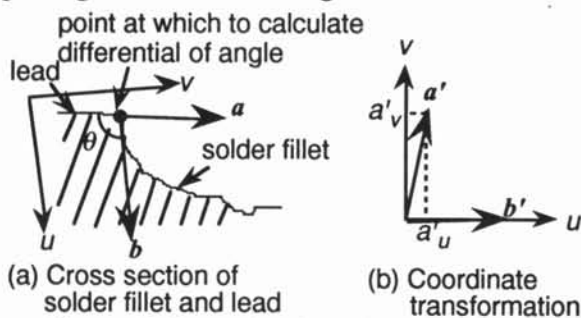


Figure 10 Determination of lead toe edge

When flux is present on the PCB surface, pad edges are very indistinct. Therefore, these edges are detected based on the second derivative of the height image. The second derivative is determined at two points separated by a distance equal to design pad width, as shown in Figure 11 (d). These points are scanned from left to right in order to find the points where the sum of the second derivatives reaches a maximum. Pad edges are determined to exist at these positions provided that both points are lower than the threshold height.

Pad height is detected from a height image of a region within the detected pad region. In order to determine actual pad height without influence of the solder fillet, a histogram calculation window is designated such that a smaller fillet area is included in the window. If the window is designated at a location distant from the lead toe, it may straddle the pad region and the histogram would include PCB substrate height. Therefore, the fillet shape is analyzed in order to locate the window around the toe of the solder fillet. Pad height is recognized as a peak of the histogram.

(C) Fillet extraction

Since fillet shape is usually very gentle at the toe, simple comparison of fillet height with pad height is insufficient for accurate detection of the fillet toe. Fillet height decreases with increasing distance from the lead toe, whereas pad area remains relatively constant. Thus, the fillet toe is determined as the position where the height is close to the pad height and the height gradient becomes non-negative. The portion whose height exceeds pad height and which is located between the lead toe and the fillet toe is recognized as being the solder fillet.

Following extraction of the fillet, the solder joint is evaluated according to the inspection criteria shown in Figure 5. Approximately 10 inspection parameters are used for the defect judgment algorithm described above. Almost all image processing parameters can be determined based on design data of component and judgment criteria are understandable physical values. Therefore, these parameters and the criteria do not have to be modified even when the soldering conditions are changed.

5. Automated inspection system

Figure 12 shows the external appearance of the developed automated system. The acquired image is distributed to three image processing RISC boards, which perform parallel processing. The entire inspection algorithm is installed on the RISC boards, which are arranged on a PC/AT. A VME bus-based microcomputer system is connected to the PC/AT by ethernet and is used for

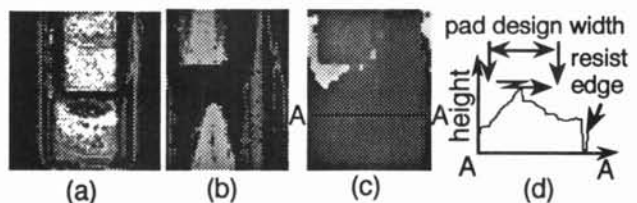


Figure 11: (a) Intensity image of visible pad. (b) Intensity image of invisible pad. (c) Height image of (b). (d) Cross section profile of (c).

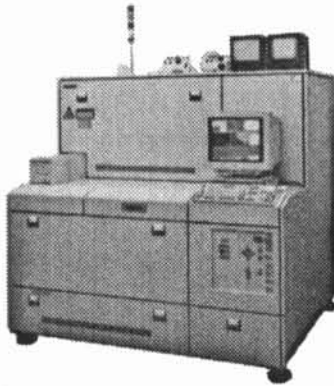


Figure 12 External appearance of the developed system

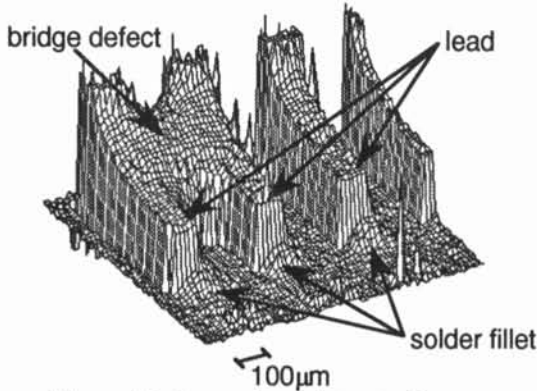


Figure 13 Example of detected image (0.3mm pitch QFP)

management of inspection data and control of the XYZ stage on which an inspection target board is mounted.

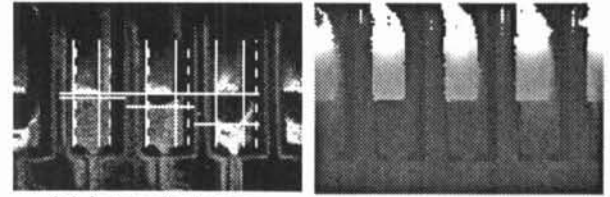
6. Evaluation of the inspection system

Figure 13 shows an example of the detected height image of 0.3mm pitch leads of a QFP. The solder fillet is clearly detected even though its volume is very small and fillet height is as low as 50µm.

The performance of the system was evaluated using PC boards in an actual production line. Figure 14 shows example defects detected in 0.5mm pitch QFP leads; "no connection" and "insufficient solder". Figure (a) shows the intensity image of the lead and Figure (b) the height image. Figure (a) shows the superimposed images of the lead edges, pad edges and toe position of the solder fillet, which are recognized by the developed algorithms. Notice that all of these were detected correctly. Evaluation results are summarized in Table 1. The inspected components consist of 0.3-1.0mm lead pitch QFPs, 1.27-2.54mm lead pitch SOPs and chip components of various sizes such as 1608 and 2125, and large part of these components were covered with flux. The developed system realizes a 100%(76/76) defect detection rate and a 0.16% (74 / 47,218) false alarm rate.

7. Conclusion

The present authors have developed a new automated visual inspection system used for solder joints of surface mount devices. A height image is acquired by a newly developed height sensor using a principle of the confocal microscope. A developed inspection algorithm classifies



(a) Intensity image (b) Height image

Figure 14 Example of detected defects

Table 1. Evaluation results

Items	results
Inspected components	SOP, QFP, Chip, X-PAK
Defect detection rate	100% (76/76)
False alarm rate	0.16% (74/47,218)

solder joints based on three-dimensional shape analysis. In order to realize stable recognition without being influenced by erroneous height data resulting from insufficient light reflected from the steep portion of a solder fillet, the present authors have developed a unique noise reduction algorithm utilizing a model shape of the solder joint, as well as a statistical edge detection algorithm based on the highest probability of edge location. Results of evaluation of the developed system confirm that it realized a 100% defect detection rate and a 0.16% false alarm rate. These results show that the system shows promises as being usable in an actual production line.

References

- [1] T. Hiroi *et al.*, "Development of Solder Joint Inspection Method using Air Stimulation Speckle Vibration Detection Method and Fluorescence Detection Method", MVA'92, pp. 429-434 (Dec. 1992, Tokyo)
- [2] R. Vanzetti *et al.*, "Automated Laser Inspection of Solder Joints", ISTFA, pp. 85-96 (1981)
- [3] J. A. Adams, "Inspection of Fine-Pitch Technology for Solder Quality using Scanned-Beam Laminography", proceedings of ISHM'90, pp. 378-388 (1990, Illinois)
- [4] A. Gieles and W. Venema, "Inspection of SMD's with 3-D Laser Scanning", Vision'89, pp. 5.59-5.71 (Apr. 1989)
- [5] S. L. Bartlett *et al.*, "Automatic Solder Joint Inspection", IEEE Trans. PAMI Vol.10, No.1, pp. 31-43 (Jan. 1988)
- [6] Y. Takagi *et al.*, "Visual Inspection Machine for Solder Joints Using Tiered Illumination", SPIE Vol.1386 Machine Vision Systems Integration in Industry, pp. 21-29 (1990, Massachusetts)
- [7] S. Kobayashi *et al.*, "Identifying Solder Surface Orientation from Color Highlight Images", IECON'90, pp. 821-825 (Nov. 1990, California)
- [8] T. Muraoka and C. Rice, "Applications of Laser Systems in Post Solder Inspection Equipment", IECON'90, pp. 805-810 (Nov. 1990, California)
- [9] J. Yano *et al.*, "3-D Visual Inspector of PCB using Laser", IECON'90, pp. 811-814 (Nov. 1990, California)